Dalton Transactions

ROYAL SOCIETY OF CHEMISTRY

PAPER

View Article Online
View Journal | View Issue

Check for updates

Cite this: *Dalton Trans.*, 2025, **54**, 6563

Changing the properties of monodentate and P,C-chelating ferrocenyl-substituted 1,2,3-triazol-5-ylidene ligands through an inserted carbonyl moiety†

Věra Varmužová, Ivana Císařová and Petr Štěpnička *

Received 6th March 2025,
Accepted 21st March 2025

DOI: 10.1039/d5dt00545k

rsc.li/dalton

Triazolylidenes derived from readily accessible triazoles are useful ligands for coordination chemistry and catalysis. This work describes the synthesis of Group 11 metal complexes of new ferrocenyl-substituted triazolylidene ligands in which the ferrocene and triazolylidene moieties are separated by a carbonyl linker. In particular, complexes of types [MCl(FcC(O){CCN(Mes)NN(Me)}-κC^5)] (M = Cu or Au; Fc = ferrocenyl) and [M(FcC(O){CCN(Mes)NN(Me)}-κC^5)$_2$][BF_4] (M = Cu, Ag, or Au) were prepared from FcC(O)C≡CH and characterised by spectroscopic methods, X-ray diffraction analysis and cyclic voltammetry. Using a similar strategy, the Pd(II) complex *trans*-[$PdCl_2$(Ph_2PfcC(O){CCN(Mes)NN(Me)}-κ^2P,C^5)] (fc = ferrocene-1,1′-diyl) was synthesised and analogously characterised. The phosphinocarbene ligand in this compound coordinates as a *trans* P,C-chelating ligand, unlike its analogues that lack the C=O spacer and similar compounds that combine the phosphine and carbene donor groups on the ferrocene scaffold. The influence of the carbonyl spacer was evaluated in a pair of Pd(II) bis-carbene complexes, [$PdBr_2$({C(Fc)CN(Mes)NN(Me)}-κC^5)(iPr_2-bimy)] and [$PdBr_2$(FcC(O){CCN(Mes)NN(Me)}-κC^5)(iPr_2-bimy)] (iPr_2-bimy = 1,3-diisopropyl-1,3-dihydro-2*H*-benzimidazol-2-ylidene), by Huynh's electronic parameters and the Fe^{II}/Fe^{III} redox potential from cyclic voltammetry, which suggested an electron density decrease at the ferrocenyl group and decreased σ donor ability of the triazolylidene moiety upon introduction of the C=O linker. The Group 11 metal complexes were tested as catalysts for the metal-catalysed cyclisation of *N*-propargylbenzamide into 2-phenyl-5-methylene-4,5-dihydrooxazole. Among them, the chlorogold complex activated with a silver salt achieved the best results.

Introduction

During the decades that have passed since the early studies by Wanzlick[1] and Öfele[2] in the 1960s[3] and the isolation of the first 1,3-dihydro-2*H*-imidazol-2-ylidene in 1991,[4,5] heteroatom-stabilised carbenes have evolved into useful ligands for coordination chemistry and catalysis by transition metal complexes, efficient organocatalysts[6] and versatile reagents.[7] In parallel, the family of these compounds has been vastly expanded from imidazole-based carbene to analogues derived from other heterocycles.[6]

Of particular interest in this area are 1,2,3-triazol-5-ylidenes, which were first reported in 2008,[8] as examples of so-called abnormal or mesoionic carbenes[9] (Scheme 1). Their attractiveness lies mainly in the facile synthesis of their precursor 1,2,3-triazoles[10] and the possibility of nearly limitless modifications through the attached substituents that, in turn, allow for fine-tuning according to the purpose.[11]

The compounds of this type that are relevant to the present work are ferrocenyl-substituted 1,2,3-triazol-5-ylidenes (**A** and **B** in Scheme 2),[12,13] which have been studied as redox-active and redox-switchable ligands[14] and further utilised as ligands in asymmetric catalysis[15] and Au(I) complexes with anticancer activity.[16]

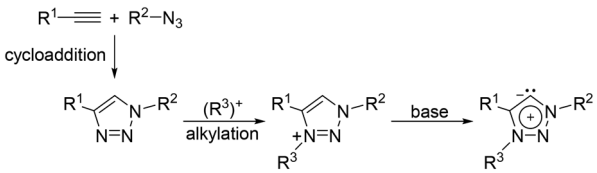

Scheme 1 General synthesis of 1,2,3-triazol-5-ylidenes (only one of the triazole regioisomers is shown for clarity).

Department of Inorganic Chemistry, Faculty of Science, Charles University, Hlavova 2030, 128 40 Prague, Czech Republic. E-mail: stepnic@natur.cuni.cz

†Electronic supplementary information (ESI) available: Complete experimental details, crystallographic data and structure diagrams, additional cyclic voltammograms, and copies of the NMR spectra. CCDC 2427432–2427441. For ESI and crystallographic data in CIF or other electronic format see DOI: https://doi.org/10.1039/d5dt00545k

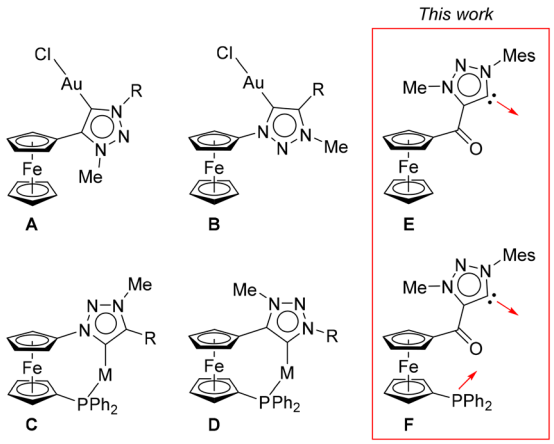

Scheme 2 Representative examples of complexes with ferrocenyl-substituted 1,2,3-triazol-5-ylidene ligands (**A**: R = Mes, 2,6-diisopropylphenyl or ferrocenyl; **B**: R = Ph or alkyl; **C** and **D**: R = CH_2Ph, Mes) and the ligands aimed at in this work (**E** and **F**: Mes = mesityl).

In all these compounds, however, the ferrocenyl groups are attached *directly* to the triazolylidene ring; complexes with spacer groups between the triazolylidene and ferrocene moieties have not been synthesised thus far.[17] Therefore, in continuation of our studies focused on the coordination chemistry of (phosphino)ferrocenyl carbene ligands,[18] we aimed to synthesize triazolylidene complexes with ferrocenyl carbonyl substituents[19] (Scheme 2). The inserted carbonyl group in the targeted compounds was expected to alter both the donor and stereochemical properties of the carbene ligands by masking the strong electron-donating ability of the ferrocene unit and increasing the overall molecular flexibility, respectively, as noted for ferrocene acylphosphines.[20] A further impetus for the present work was a literature survey which showed that complexes with 4-acyltriazolylidene ligands have most likely not yet been reported.[21]

In addition to monodentate acyltriazolylidene ligands (**E** in Scheme 2), we have focused on related phosphinotriazolylidene **F** that expands the family of structurally attractive, P,C-chelating phosphinoferrocene carbene ligands[22] and complements the previously studied type **C** and **D** donors (Scheme 2).[18c]

This work describes the synthesis and detailed structural characterisation of Group 11 metal complexes with ligand **E** and a Pd(II) complex with P,C-chelating ligand **F**. Additionally, the results of the catalytic evaluation of the former complexes in the model cyclisation of *N*-propargyl benzamide are presented.

Results and discussion

Synthesis and characterisation of complexes with monodentate acyltriazolylidene ligands

The triazolium salt required for the preparation of ferrocenylcarbonyl-substituted 1,2,3-triazol-5-ylidene complexes (**E** in Scheme 2) was obtained from alkynyl ketone **1**[23] (Scheme 3). In the first step, the ketone was subjected to a Cu-catalysed reaction with mesityl azide to produce triazole **2**. The cycloaddition reaction, which was performed in the presence of CuI (20 mol%) and diisopropylethylamine (2 equiv.)[24] for 4 h, proceeded cleanly and provided the triazole in an 87% isolated yield. The use of only 1 equiv. of the amine and 10 mol% copper(I) salt resulted in incomplete conversion, whereas longer reaction times led to partial decomposition.

Triazole **2** was subsequently methylated with Meerwein salt in dichloromethane to afford the desired triazolium salt **3** (82% yield); no alkylation was observed with methyl iodide in

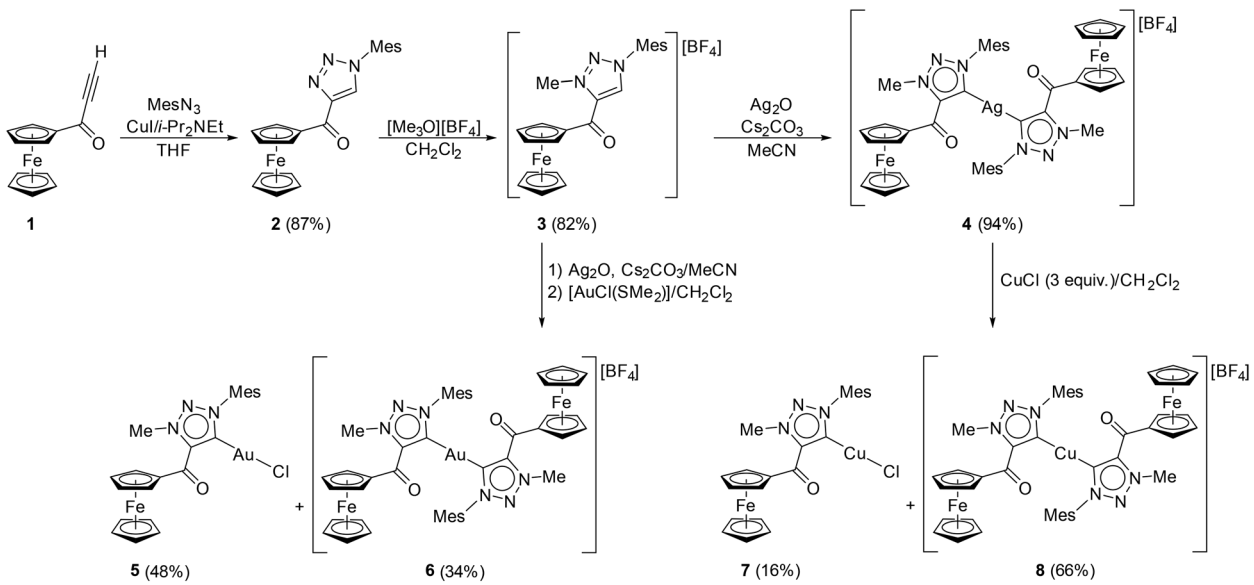

Scheme 3 Synthesis of triazolium salt **3** and its conversion into carbene complexes **4**–**8** (Mes = mesityl).

MeCN, even at an elevated temperature (3 equiv. of MeI, 60 °C, overnight).

Both intermediates were fully characterised by NMR and IR spectroscopy, electrospray ionisation (ESI) mass spectrometry and elemental analysis. The formation of the triazole ring was indicated by the characteristic signals due to the triazole C═CH moiety (**2**: ═CH, δ_H 8.23 and δ_C 128.58; ═C, δ_C 148.90). Upon alkylation, these signals shifted (**3**: ═CH, δ_H 8.85 and δ_C 132.48; ═C, δ_C 138.54), and an additional signal due to the methyl substituent emerged in the spectra (δ_H 4.68 and δ_C 41.66). The presence of the tetrafluoroborate anion was corroborated by an intense band attributable to the $\nu_3(BF_4^-)$ mode[25] centred at ≈1054 cm^{-1} in the FTIR spectra and by the ^{19}F NMR spectra showing a pair of resonances at $\delta_F \approx -152$ attributable to the $^{10}BF_4^-$ and $^{11}BF_4^-$ isotopomers in a 1 : 4 ratio.

The molecular structures of **2** and **3** are presented in Fig. 1. The latter compound crystallised as a hemihydrate **3**·½H_2O with two triazolium cations, two partially disordered anions and one water molecule in the asymmetric unit. The multiplication of the structurally independent "molecules"[26] can be ascribed to the presence of adventitious water in a substoichiometric amount and its role in intermolecular interactions, as well as to the chirality of the crystal assembly (space group $P2_1$; see ESI†).

The bond lengths within the triazole ring of **2** (Table 1) compare well with parameters reported for the compound without the C═O spacer, 4-ferrocenyl-1-mesityl-1*H*-1,2,3-triazole.[14a] The triazole ring is planar and oriented with its CH moiety towards the C═O bond (torsion angle C1–C2–C3–O1: 18.2(2)°). The cyclopentadienyl ring and the triazole unit are mutually twisted by 26°, and the bulky mesityl substituent is nearly perpendicular to the triazole plane.

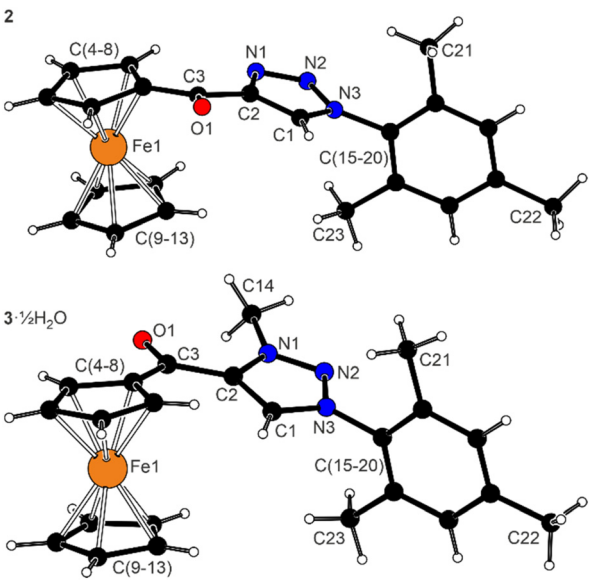

Fig. 1 Molecular structures of **2** (top) and cation 1 in the structure of **3**·½H_2O (bottom). For displacement ellipsoid plots and additional structure diagrams, see the ESI.†

Table 1 Selected distances and angles for **2** and **3**·½H_2O (in Å and °)

Parameter[a]	**2**	**3**·½H_2O (mol 1)[b]	**3**·½H_2O (mol 2)[b,c]
C1–C2	1.374(2)	1.375(3)	1.378(3)
C2–N1	1.369(1)	1.371(3)	1.366(3)
N1–N2	1.307(1)	1.313(3)	1.311(3)
N2–N3	1.364(1)	1.330(3)	1.328(3)
N3–C1	1.339(1)	1.353(3)	1.351(3)
Fe–C	2.026(1)–2.068(1)	2.026(2)–2.053(2)	2.013(2)–2.075(2)
tilt	4.84(7)	1.7(2)	1.8(2)
C3–O1	1.229(1)	1.222(2)	1.228(3)
C2–C3–C4	120.8(1)	120.0(2)	119.2(2)
tz *vs.* Cp	26.18(7)	23.0(1)	21.6(1)
tz *vs.* Mes	82.28(6)	87.6(1)	81.7(1)

[a] Definitions: Fe–C is the range of the ten Fe–C bonds in the ferrocene unit; tilt is the dihedral angle of the cyclopentadienyl ring planes; tz *vs.* Cp and tz *vs.* Mes are the interplanar angles between the triazole ring and the cyclopentadienyl C(4–8) ring and mesityl plane C(15–20), respectively. [b] Further data: N1–C14 1.473(3) in molecule 1 and 1.471 (3) in molecule 2. [c] The atom numbering in molecule 2 is strictly analogous to that in molecule 1.

The two independent cations in the structure of **3**·½H_2O show only minor conformational differences. The changes in the bond lengths within the triazole ring upon alkylation are small, with the most pronounced differences being shortening of the N2–N3 bond and elongation of the N3–C1 bond; the bonds to N1, at which the methyl group was introduced, remain virtually unchanged. The mutual orientation of the triazole and the two adjacent rings C(4–8) and C(15–20) in **3** is similar to that in **2**, but the central triazole ring in the salt is inverted so that its N1–C14 bond is directed to the C═O moiety (*cf.* the C1–C2–C3–O1 torsion angle: −165.5(1)° in molecule 1 and −156.2(2)° in molecule 2).

Compound **3** reacted smoothly with excess silver(I) oxide and caesium carbonate[14a,b,d] in acetonitrile at ambient temperature to produce deep red bis-carbene complex **4** in a practically quantitative yield (94% isolated yield; Scheme 3). A similar reaction without[27] carbonate (as an additional base) proceeded with incomplete conversion of the starting material. The reaction performed in the presence of KCl to obtain a chlorosilver(I) monocarbene complex also furnished **4** as the sole product.[16]

The formation of complex **4** was indicated by a low-field carbene resonance at δ_C 171.87 that was split into a pair of concentric doublets by ^{107}Ag and ^{109}Ag (both $I = \frac{1}{2}$, ≈1 : 1 ratio), with coupling constants ($^1J_{AgC}$ = 171 and 197 Hz) proportional to the gyromagnetic ratios of the isotopes. A similar albeit smaller splitting was observed for the more distant triazolylidene CH signal ($^2J_{AgC}$ = 14 and 16 Hz), whereas the C═O signal shifted to a lower field to a position close to that determined for triazole **2** (*cf.* δ_C 189.04, 183.49 and 188.95 for **2**, **3** and **4**, respectively).

The addition of [AuCl(SMe$_2$)] (1 equiv. relative to **3**) to the *in situ*-generated **4** resulted in smooth transmetalation,[28] which led to a separable mixture of the mono- and bis-carbene Au(I) complexes **5** and **6** as intensely violet solids in 48% and 34% yields, respectively (Scheme 3). As judged from the NMR

spectra, a minor amount of another carbene complex (δ_C 174.19) was present in the crude mixture, which, unfortunately, could not be isolated.

Attempts to synthesise Cu(I) carbenes directly from salt **3** (by reacting **3** with either Cu_2O, KCl and Cs_2CO_3 in MeCN at 80 °C or CuCl, K_2CO_3 and $(PhCH_2NEt_3)Cl$ in acetone at 60 °C) were unsuccessful. Gratifyingly, transmetalation[29] using **4** and freshly prepared CuCl produced the targeted compounds, again as a mixture of the mono- and bis-carbene complexes **7** and **8**, with the latter dominating irrespective of the amount of CuCl applied (1 or 3 equiv.). The complexes were isolated by chromatography and obtained as deep violet solids in 16% and 66% yields, respectively (from the reaction with 3 equiv. of CuCl).

The NMR spectra of **5–8** were generally similar to those of **4** and consistent with the proposed structures. The characteristic carbene ^{13}C NMR signals were detected at δ_C 162.12 and 174.27 for **5** and **6**, respectively, and at δ_C 168.61 and 168.45 for **7** and **8**, respectively.

All the carbene complexes were structurally authenticated by single-crystal X-ray diffraction analysis. The bis-carbene complexes **4** and **6** crystallised as isostructural solvates **4**·CH_2Cl_2 and **6**·CH_2Cl_2; the analogous copper(I) complex was isolated as acetone solvate **8**·Me_2CO with a very similar overall geometry. The molecular structure of the representative compound **4**·CH_2Cl_2 is shown in Fig. 2; selected geometric data for all complexes are presented in Table 2 (further structural diagrams and geometric parameters are available in the ESI†).

The crystal structures of **4**·CH_2Cl_2, **6**·CH_2Cl_2 and **8**·Me_2CO reveal symmetrical linear coordination around the metal ions (C–M–C = 174–176°), with the M–C distances increasing from Cu to Au to Ag, in line with the trend in the covalent radii of the metals (albeit not linearly, see the ESI; Fig. S9†)[30] and influenced by relativistic effects for gold.[31] The two M–C distances in individual compounds are identical within the margins of experimental uncertainty and do not depart from the values reported for similar molecules.[16,32] Compared with precursor **3**, the triazolylidene rings present slightly elongated C1–C2 and C1–N3 distances (approximately 0.010–0.015 Å); the remaining in-ring distances are virtually unchanged.

Notably, the complex cations have the same arrangement, with the ferrocene units on one side and the mesityl substituents on the other. The mesityl groups are nearly perpendicular to the central triazolylidene plane, whereas the substituted cyclopentadienyl rings are twisted by approximately 44°. The C═O and N–Me bonds point in the same direction and are oriented similarly to those in **3** (the C1–C2–C3–O1 dihedral angles were ≈140° in all the complexes).

Monocarbene complexes **5** and **7** were isostructural (Fig. 3). An inspection of the geometric parameters (Table 3) reveals longer M–Cl and M–C bonds for the Au(I) complex, in agreement with the larger size of this metal ion and the trends observed for complexes [LMCl], where L = 1,4-bis(2,6-diisopropylphenyl)-3-methyl-1,2,3-triazol-5-ylidene and M = Cu or Au.[33] The M–C bonds in **5** and **7** are shorter than those in the corresponding bis-carbene complexes, in line with a lower

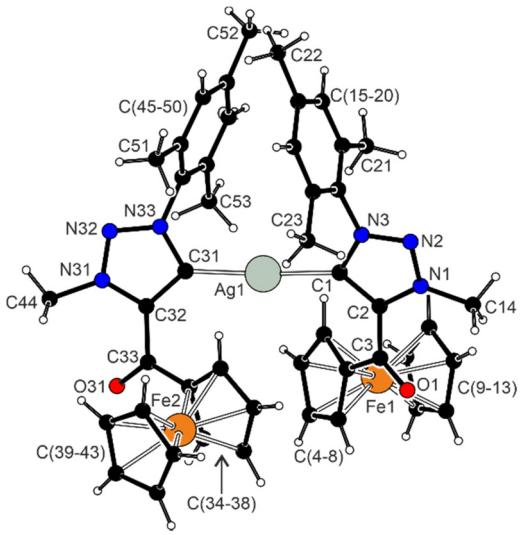

Fig. 2 Complex cation in the structure of **4**·CH_2Cl_2 (displacement ellipsoid plot is available in the ESI†).

Table 2 Selected distances and angles for bis-carbene complexes **8**·Me_2CO, **4**·CH_2Cl_2 and **6**·CH_2Cl_2 (in Å and °)

Parameter[a]	**8**·Me_2CO (M = Cu)		**4**·CH_2Cl_2 (M = Ag)		**6**·CH_2Cl_2 (M = Au)	
M1–C1/31	1.898(1)	1.899(1)	2.074(1)	2.075(1)	2.014(2)	2.014(2)
C1–M1–C31	175.74(6)		174.42(5)		176.25(7)	
tz *vs.* tz	34.87(8)		35.67(8)		35.3(1)	
C1–C2/C31–C32	1.392(2)	1.391(2)	1.386(2)	1.389(2)	1.384(2)	1.386(2)
C2–N1/C32–N31	1.369(2)	1.366(2)	1.370(2)	1.368(2)	1.367(2)	1.365(2)
N1–N2/N31–N32	1.310(2)	1.305(2)	1.308(2)	1.309(2)	1.306(2)	1.311(2)
N2–N3/N32–N33	1.336(2)	1.334(2)	1.335(2)	1.340(2)	1.333(2)	1.337(2)
N3–C1/N33–C31	1.368(2)	1.367(2)	1.367(2)	1.363(2)	1.367(2)	1.366(2)
Fe–C range	2.036(2)–2.059(2)	2.034(1)–2.055(2)	2.032(1)–2.058(2)	2.038(2)–2.059(2)	2.031(2)–2.056(2)	2.036(2)–2.057(2)
tilt	2.8(1)	2.32(8)	1.93(8)	2.41(9)	2.3(1)	2.8(1)
C3–O1/C33–O31	1.226(2)	1.225(2)	1.227(2)	1.225(2)	1.226(2)	1.224(2)
C1–C2–C3–O1	143.5(2)	140.4(2)	−141.7(2)	−142.2(1)	−139.6(2)	−140.7(2)
tz *vs.* Cp	44.00(8)	46.36(8)	46.53(8)	45.99(8)	47.6(1)	46.7(1)
tz *vs.* Mes	81.19(7)	88.83(7)	86.14(7)	77.34(7)	86.49(9)	78.01(9)

[a] The parameters are defined as for precursors **2** and **3**; see the footnote to Table 1.

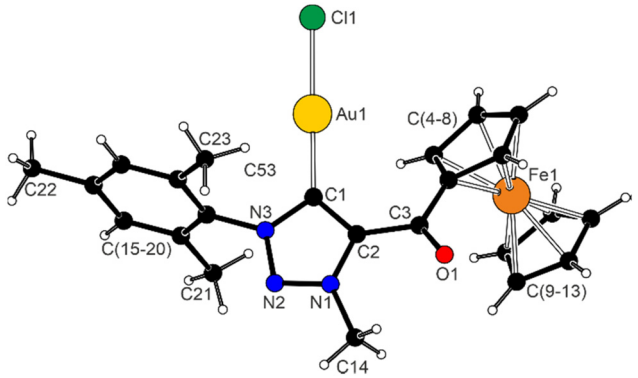

Fig. 3 Molecular structure of complex **5** (for additional structure diagrams and conventional displacement ellipsoid plots, see the ESI†).

Table 3 Selected distances and angles for complexes **5** and **7** (in Å and °)

Parameter[a]	**5** (M = Cu)	**7** (M = Au)
M1–Cl1	2.1003(6)	2.2790(5)
M1–C1	1.876(2)	1.985(2)
Cl1–M1–C1	174.48(6)	177.30(5)
C1–C2	1.398(2)	1.394(2)
C2–N1	1.367(2)	1.365(2)
N1–N2	1.310(2)	1.310(2)
N2–N3	1.336(2)	1.338(2)
N3–C1	1.373(2)	1.368(2)
Fe–C	2.028(2)–2.053(2)	2.031(2)–2.049(2)
tilt	0.8(1)	1.4(1)
C3–O1	1.225(2)	1.226(2)
C1–C2–C3–O1	155.0(2)	152.0(2)
tz *vs.* Cp	35.5(1)	41.1(1)
tz *vs.* Mes	69.8(1)	76.00(9)

[a] The parameters are defined as for precursors **2** and **3**; see footnote to Table 1.

trans-influence of the chloride ligand.[34] While the geometry of the carbene ligands does not differ from that of the bis-carbene complexes, **5** and **7** show smaller dihedral angles between the triazolylidene moiety and the adjacent rings (cyclopentadienyl and mesityl), which is indicative of reduced steric crowding around the metal centres ligated by only one bulky carbene donor; the parameters of the triazolylidene units are virtually the same, and even the substituents at the triazolylidene moiety are similarly oriented.

The carbene complexes and their common precursor **3** were studied by cyclic voltammetry at a glassy carbon disc electrode in dichloromethane that contained 0.1 M $Bu_4N[PF_6]$ as the supporting electrolyte. In the accessible potential range, salt **3** displayed single reversible oxidation at 0.35 V *vs.* the ferrocene/ferrocenium reference,[35] which was attributed to one-electron oxidation of the ferrocene unit (Fig. 4). In the cathodic region, the compound underwent reversible one-electron reduction at −1.56 V, followed by an additional irreversible redox event at approximately −2.1 V (the anodic peak potential at a 100 mV s^{-1} scan rate is given). A generally similar behaviour and redox potentials were reported for a compound in which the redox-active ferrocenyl group was attached directly to the triazolium ring.[14a,e]

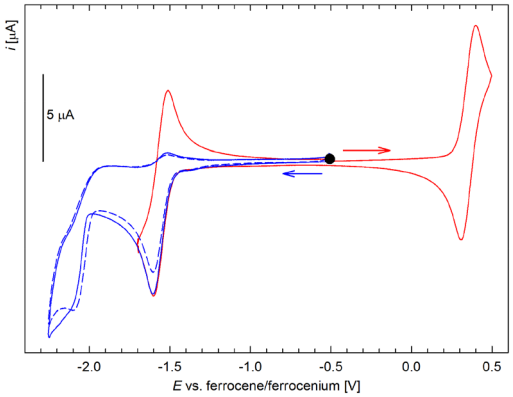

Fig. 4 Cyclic voltammograms of triazolium salt **3** (recorded in 0.1 M $Bu_4N[PF_6]/CH_2Cl_2$ at a glassy carbon disc electrode and a 100 mV s^{-1} scan rate).

Under similar conditions, monocarbene complex **5** showed reversible oxidation at 0.26 V and reversible reduction at −2.06 V (Fig. 5). The shift of the oxidative wave to a lower potential than that of **3** can be explained by the loss of positive charge, which makes the azole substituent less electron-withdrawing (maybe also due to backdonation from Au) and may lower the coulombic barrier for electron removal.

The redox responses of bis-carbene complexes **4**, **6** and **8** were different: Cu(I) complex **8** displayed reversible oxidation centred at ≈0.30 V (Fig. 6). The redox wave was relatively broad (with a peak separation of ≈140 mV, which was significantly greater than the ≈80–85 mV for decamethylferrocene standard under the conditions applied) and consisted of two narrowly separated one-electron waves, as corroborated by differential pulse voltammetry, which revealed two unresolved peaks (Fig. 7; full resolution of the two peaks was not achieved even by changing the modulation amplitude).[36] This behaviour can

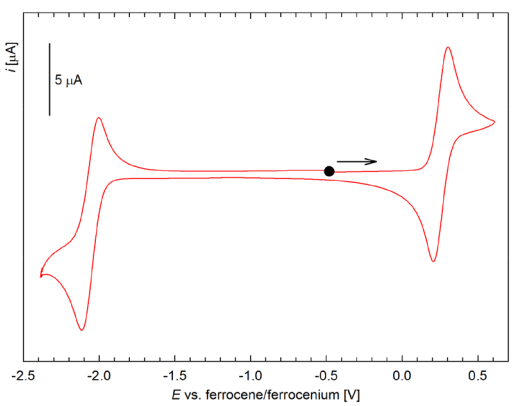

Fig. 5 Cyclic voltammogram of carbene complex **5** (recorded in 0.1 M $Bu_4N[PF_6]/CH_2Cl_2$ at a glassy carbon disc electrode and a 100 mV s^{-1} scan rate).

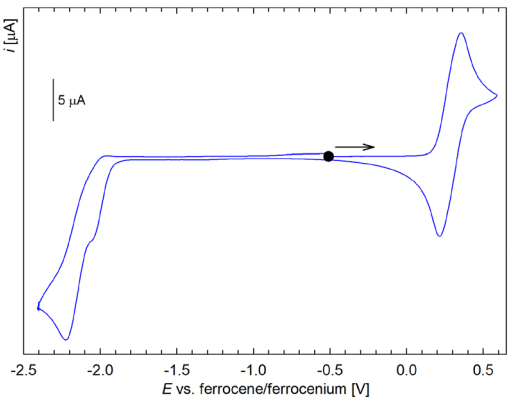

Fig. 6 Cyclic voltammogram of bis-carbene complex **8** (recorded in 0.1 M $Bu_4N[PF_6]/CH_2Cl_2$ at a glassy carbon disc electrode and a 100 mV s^{-1} scan rate).

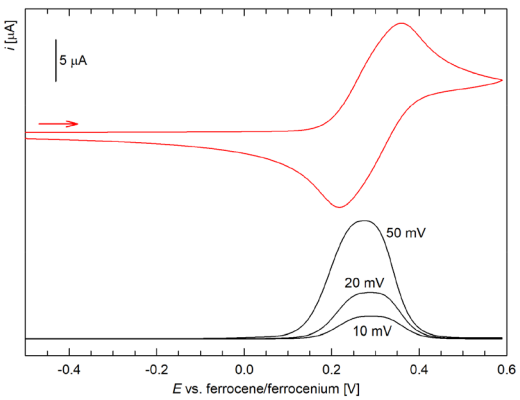

Fig. 7 Detailed cyclic (red curve) and differential pulse (black lines) voltammograms recorded for the first reversible oxidation of bis-carbene complex **8** (scan rate: 100 mV s^{-1}; the modulation amplitude is specified in the graph).

be explained by sequential oxidation of the two chemically equivalent ferrocene units, which probably do not communicate electronically but are differentiated by the first oxidation. In the cathodic region, complex **8** underwent two successive irreversible reductions at approximately −2.06 and −2.21 V (the peak potentials at a scan rate of 100 mV s^{-1} are given), which was attributable to redox changes localised at the triazolylidene units.

The redox behaviours of complexes **4** and **6** containing heavier metals were essentially similar except that their oxidation waves were less resolved (peak separation ≈105 mV), and for complex **6**, the oxidation was associated with adsorption, which gave rise to an anodic prepeak and resulted in the anodic counterwave gaining the appearance of a stripping peak when the scan range was extended towards more positive potentials (see the ESI†).

The oxidations of **4** and **6** were detected at approximately 0.28 V, and their smaller separations can be explained by longer M–C distances (M = Ag and Au), which make the ferrocene units more distant and, hence, more independent. Cathodic waves were observed at approximately −2.05 and −2.22 V for the silver complex and at −2.02 V for its Au(I) congener (the second wave could not be unambiguously localised for **6**).

Evaluation of the donor properties

The electronic properties of the acyltriazolylidene ligand **E** were evaluated from two directions: the Huynh electronic parameter (HEP)[37] was used to probe the effect of the C═O linker on the carbene donor ability, and its influence on the ferrocene unit was monitored by cyclic voltammetry. For this purpose, a pair of Pd(II) bis-carbene complexes **10** and **11** were prepared from salt **3** and its "nonspaced" analogue **9**, respectively. Compound **9** was obtained from ethynylferrocene and mesityl azide under modified conditions (see the ESI†) and subsequently alkylated according to the literature.[14a] Both salts were treated with Ag_2O in the presence of Cs_2CO_3 (in MeCN), and the presumed Ag(I)-carbene intermediate was directly transmetalated[37a,b] with $[PdBr_2(iPr_2\text{-bimy})]_2$[38] (in CH_2Cl_2; iPr_2-bimy = 1,3-diisopropyl-1,3-dihydro-2*H*-benzimidazol-2-ylidene) to produce the targeted Pd(II) bis-carbene complexes **10** and **11** in good isolated yields (≈65%; Scheme 4).

Complex **11** was orange as typical for simple ferrocene derivatives,[39] whereas compound **10**, which possesses a conjugated C═O chromophore, was intensely burgundy red. This difference was clearly manifested in the UV-vis spectra (λ_{max} = 503 nm for **10** and 450 nm for **11**; see the ESI†). In their NMR spectra, complexes **10** and **11** displayed all the expected resonances, including the set of signals due to a monosubstituted

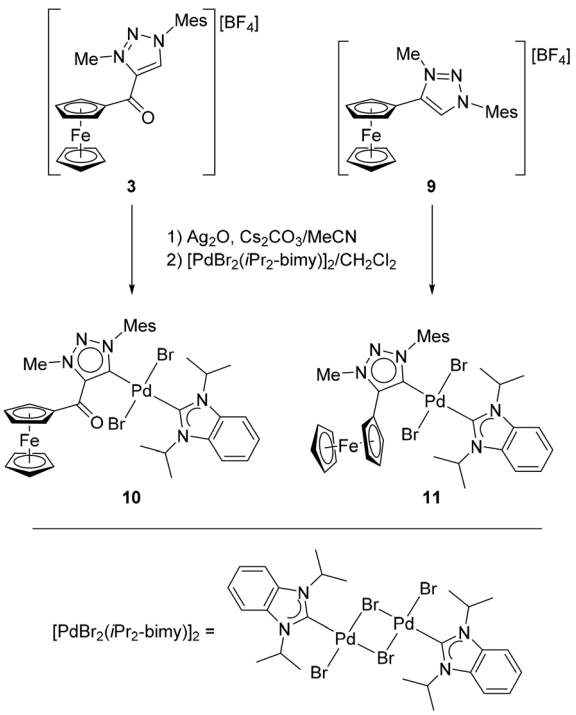

Scheme 4 Preparation of Pd(II) complexes **10** and **11**.

ferrocene unit and the iPr_2-bimy ligand; the signal of the C═O group in **10** was observed at δ_C 189.16. In addition, two carbene ^{13}C NMR signals were detected and clearly distinguished *via* 2D NMR spectra (the ^{13}C NMR signal due to iPr_2-bimy was correlated with the C*H*Me_2 proton signals). For both compounds, the triazolylidene signal was found at a higher field than the resonance of the iPr_2-bimy reporter group. The HEP values (the chemical shifts quoted here are relative to the solvent signal ($CDCl_3$) at δ_C 77.7 per the recommendation) were 177.88 ppm for **10** and 179.97 ppm for **11**, which correspond to the data obtained for similar compounds[40,14c] and suggest that the acyltriazolylidene ligand in **10** is a weaker σ donor than its analogue without the C═O spacer in complex **11**.

This observation was consistent with the information inferred from cyclic voltammetry. Complexes **10** and **11** displayed single reversible oxidations at $E^{\circ\prime}$ 0.26 and 0.12 V *vs.* ferrocene/ferrocenium, respectively (Fig. 8). The positions of the waves, which were ascribed to a ferrocene-centred, one-electron redox transition, indicated easier oxidation of **11**, even though the difference in the redox potentials was smaller than, *e.g.*, that between the redox potentials of ferrocene and benzoylferrocene (ΔE = 0.21 V in $Bu_4N[PF_6]$/MeCN).[41] In addition, the complexes underwent simple (**11**: $E \approx -2.3$ V) or multistep (**10**) irreversible reduction, similar to bis-carbene complexes **4**, **6**, and **8** (see the ESI†).

Overall, these results indicate that the carbonyl linker lowers the electron density at both parts of the ligand moiety (ferrocene and triazolylidene) and, consequently, makes the carbene ligand a weaker σ donor. The strong electron-donating effect of the ferrocenyl substituent (*cf.* Hammett constant σ_p for the ferrocenyl group: −0.18)[42] is apparently unable to efficiently cancel out the electron-withdrawing effect of the introduced carbonyl linker (*cf.* σ_p for C_6H_5 and $C_6H_5C(O)$: −0.01 and 0.43, respectively).

Catalytic experiments

Carbene complexes **4**, **5**, **6** and **8** were evaluated as catalysts for the metal-mediated cyclisation of *N*-propargylbenzamide (**12**) to 5-methyleneoxazoline **13** (Scheme 5).[43] The reactions were performed at 25 °C in CD_2Cl_2 with 3 mol% catalyst and monitored by ^1H NMR spectroscopy.

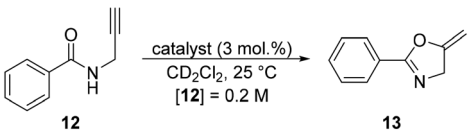

Scheme 5 Au-catalysed cyclisation of *N*-propargylbenzamide (**12**) into oxazoline **13**.

Under these conditions, no appreciable reaction was observed when bis-carbene complexes **4**, **6** and **8** were used (no product was detected after 24 h), whereas chlorogold(I) complex **5** reached only 1% conversion after a 6 h reaction time. However, when this complex was "activated" by one molar equivalent of silver bis(trifluoromethanesulfonyl)imide ($AgNTf_2$) dissolved in MeCN, a smooth reaction occurred (Fig. 9). The NMR yield of product **13** after 6 h was 97%, and the reaction followed (pseudo)first-order kinetics, as expected for a simple catalytic process. However, the performance of the **5**/$AgNTf_2$ catalyst was worse than that of the archetypal [AuCl(PPh_3)]/$AgNTf_2$ system, which achieved full conversion within 1 h under otherwise identical conditions (Fig. 9). No reaction was observed in the presence of $AgNTf_2$ only,[44] and the silver salt did not oxidize the ferrocene moiety in **5** (the addition of $AgNTf_2$ to **5** resulted in the separation of insoluble AgCl),[45] as indicated by the practically identical UV-vis spectra recorded for complex **5** and a **5**-$AgNTf_2$ (5 equiv.) mixture in dichloromethane with a little MeCN added to mimic reaction conditions (see the ESI, Fig. S64†).

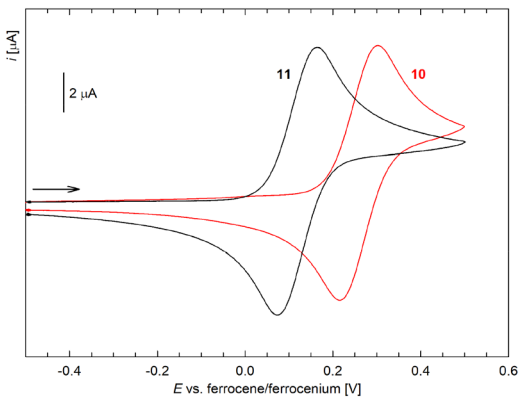

Fig. 8 Cyclic voltammograms (anodic branches) of complexes **10** and **11** (recorded in 0.1 M $Bu_4N[PF_6]/CH_2Cl_2$ at a glassy carbon disc electrode and a 100 mV s^{-1} scan rate).

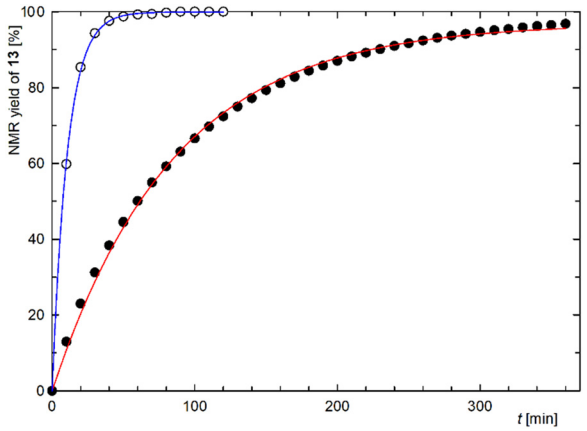

Fig. 9 Kinetic profile for the Au-catalysed cyclisation of *N*-propargylbenzamide (**12**) into methylene oxazoline **13** using **5**/$AgNTf_2$ (black circles, red line) and [AuCl(PPh_3)]/$AgNTf_2$ (empty circles, blue line) as the catalyst (conditions: 3 mol% Au, $AgNTf_2$ 1 equiv. relative to Au, dichloromethane, 25 °C). An exponential fit is shown to illustrate first-order behaviour: conversion [%] = 97.0(4) × [1 − exp(−0.0118(2)*t* [min])], r^2 = 0.9983 for **5**, and conversion [%] = 99.9(1) × [1 − exp(−0.0934(9)*t* [min])], r^2 = 0.9998 for [AuCl(PPh_3)]. The data are an average of two independent runs.

Complexes with a P,C-chelating phosphinocarbene ligand

The synthesis of analogous P,C-chelating phosphinocarbene complexes has proven more challenging. Although generally similar, it required a carefully designed sequence of synthetic steps that circumvented problems with functional group tolerance (*e.g.*, avoiding unwanted Staudinger reaction[46] between an azide and ferrocene-bound phosphine moiety or alkylation of the latter). The synthesis (Scheme 6) started from P-protected aldehyde **14**,[47] which was converted in two steps to alkynyl ketone **16** (72% yield from **14**), as described for **1**.[23] To achieve good conversion, 3 equiv. of ethynylmagnesium bromide were needed in the first step (when only 1.5 equiv. were applied, only half of the starting aldehyde reacted), and the following oxidation was performed with 20 equiv. of MnO_2. Cyclisation with mesityl azide in the presence of 20 mol% CuI and 2 equiv. of i-Pr_2NEt produced triazole **17**, which was alkylated with Meerwein salt (1.2 equiv., 2 h) to afford **18** (the isolated yields of these two steps were 90% or higher).

Attempts to remove the borane protection group[48] with methanol[49] or morpholine[50] failed (N.B. the reaction with methanol produced methyl 1′-(diphenylphosphino)ferrocene-1-carboxylate[51] as the product of C(O)-triazole bond cleavage and concomitant phosphine deprotection). Eventually, the deprotection was achieved with 1,4-diazabicyclo[2.2.2]octane[52] (dabco; 2 equiv.) in anhydrous THF overnight. Free phosphine **19** was obtained in good yield (78%) and acceptable purity by carefully optimised column chromatography and was directly converted to Pd(II) complex **20**. For this transformation, freshly prepared **19** was treated with Ag_2O and carefully dried Cs_2CO_3 in anhydrous acetonitrile, and the presumed Ag(I)-carbene intermediate was reacted without isolation with $[PdCl_2(MeCN)_2]$ in dry dichloromethane. The product was isolated by column chromatography as a deep red solid in 14% yield. Although this yield may seem disappointingly low, it corresponds to the complexity of the last reaction step.

All the compounds along the reaction sequence were fully characterised using multinuclear NMR, high-resolution mass spectrometry (MS) and elemental analysis. The collected data corroborated the proposed structures and were consistent with the data obtained for the nonphosphinylated compounds discussed above. In addition, the structures of **15** and **17** were determined *via* single-crystal X-ray diffraction analysis.

Compound **15** (Fig. 10) crystallised with the symmetry of the monoclinic space group $P2_1/n$, forming a supramolecular assembly based on ≡C–H···O interactions and O–H···HB dihydrogen bonds that involve polarised BH hydrogens as acceptors (see ESI†);[53] O–H···O interactions operating in the structures of ferrocenylmethanol[54,55] and its phosphinylated derivatives[56] were not detected.

The molecule of **15** comprises a regular ferrocene unit (tilt angle: 1.6(2)°) whose substituents assume an intermediate conformation (τ = −97.6(2)°; τ is the torsion angle C1–Cg1–Cg2–C6, where Cg1 and Cg2 are the centroids of cyclopentadie-

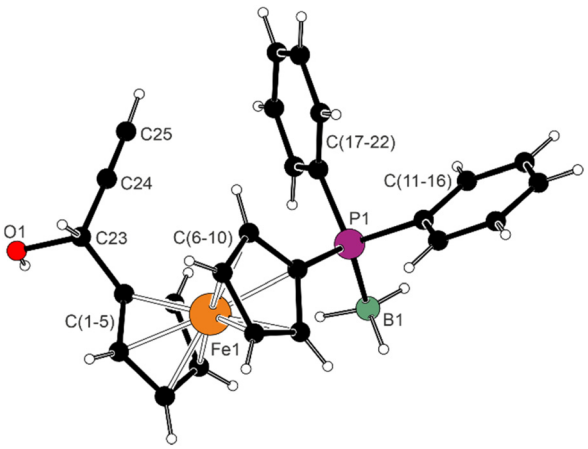

Fig. 10 Crystal structure of **15**. Selected distances and angles (in Å and °): Fe–C (range) 2.035(3)–2.057(3), P1–B1 1.927(3), P1–C6 1.789(3), P1–C11 1.823(2) P1–C17 1.811(3), C1–C23 1.497(4), C23–O1 1.441(3), C1–C23–O1 110.8(2), C23–C24 1.478(4), C24–C25 1.189(4), and C23–C24–C25 178.4(3). Displacement ellipsoid plot is available in the ESI.†

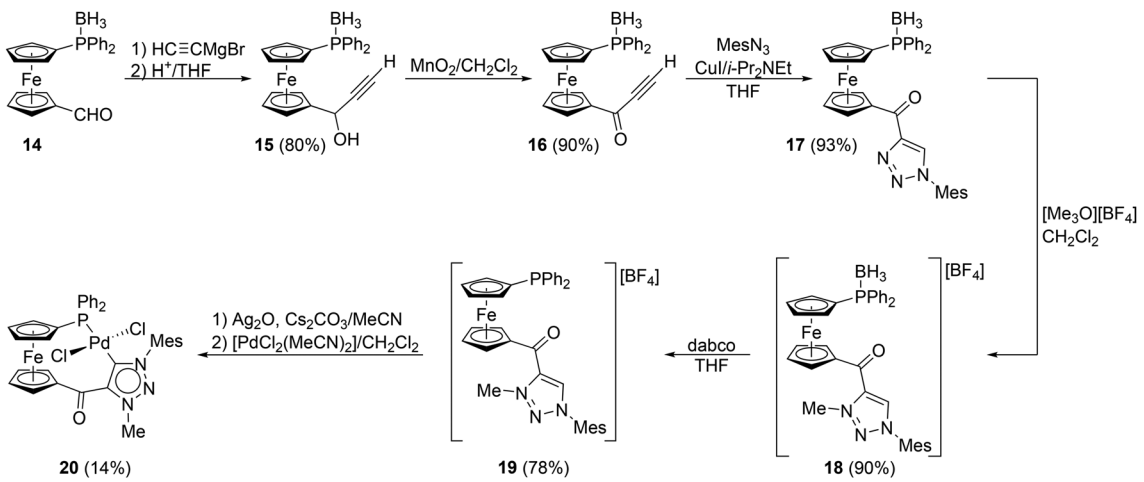

Scheme 6 Synthesis of P,C-chelating phosphinocarbene complex **20**.

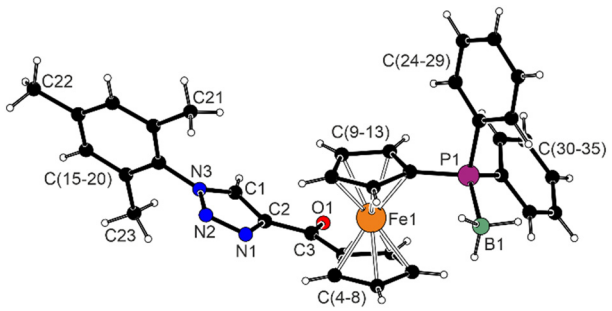

Fig. 11 Molecule **1** in the crystal structure of **17**. Selected distances and angles for molecule 1 [molecule 2] (in Å and °): Fe–C (range) 2.016(2)–2.058(2) [2.024(2)–2.065(2)], P1–B1 1.930(2) [1.919(2)], P1–C9 1.794(2) [1.798(2)], P1–C24 1.814(2) [1.812(2)], P1–C30 1.812(2) [1.811(2)], C3–O1 1.228(2) [1.225(2)], C1–C2 1.373(3) [1.371(2)], C2–N1 1.368(3) [1.364(2)], N1–N2 1.302(2) [1.305(2)], N2–N3 1.364(2) [1.357(2)], and N3–C1 1.339 (3) [1.339(2)]. A displacement ellipsoid plot is available in the ESI.†

nyl rings C(1–5) and C(6–10), respectively); the individual geometric parameters match those determined for $Ph_2PfcCH_2OH{\cdot}BH_3$ (fc = ferrocene-1,1′-diyl).[53]

Triazole **17** (Fig. 11) crystallised with two molecules in the asymmetric unit (space group $P2_1/c$), which show negligible differences, *e.g.*, in the orientations of the "terminal" phenyl rings (see the ESI†). The substituted ferrocene units are tilted by 3.1(1)° in molecule 1 [3.2(1)° in molecule 2] and adopt a 1,3′ conformation[57] characterised by τ[58] angles of −145.5(1)° [147.3(1)°]. The dihedral angle between the planes of the triazole and carbonyl-substituted cyclopentadienyl rings is 24.5 (1)° [27.3(1)°]. Otherwise, the geometries of the acyltriazole and $-PPh_2{\cdot}BH_3$ groups are unexceptional considering the data for the compounds discussed above.

Compound **20**, which represents the ultimate synthetic goal, was characterised as a structurally unique Pd(II) complex that features a phosphinocarbene ligand coordinating as a *trans* P,C-chelating donor. Notably, typical ligands capable of traversing *trans* positions in the coordination sphere of soft transition metals are symmetrical diphosphines with rigid organic backbones,[59] whereas their donor-unsymmetric counterparts remain rare.[60]

A hint for the particular arrangement, which was later corroborated by structure determination, was initially provided by the NMR spectra showing an unusually large ^{13}C–^{31}P scalar coupling constant for the carbene resonance (δ_C 157.68, $^2J_{PC}$ = 195 Hz), in the range reported for complexes *trans*-[$PdCl_2(PR_3)$(IPr)] (R = Ph, *o*-tolyl, or cyclohexyl; IPr = 1,3-bis(2,6-diisopropylphenyl)-1,3-dihydro-2*H*-imidazol-2-ylidene-κC^2; $^2J_{PC}$ = 180–200 Hz).[61] Analogous complexes that contain *cis*-chelating ferrocene phosphinocarbene ligands of types **C** and **D** (Scheme 2)[18c] and their diaminocarbene analogues[18b] presented $^2J_{PC}$ coupling constants below 10 Hz.

Furthermore, the fixed geometry rendered the ferrocene CH groups in **20** diastereotopic and, hence, eight resonances due to these groups were observed in both the ^1H and $^{13}C\{^1H\}$ NMR spectra as relatively broad signals due to structural dynamics. The C=O group resonated at δ_C 191.34, and the signal of the bonding triazole carbon was detected at δ_C 142.87 as a ^{31}P-coupled doublet ($^3J_{PC}$ = 7 Hz). The $^{31}P\{^1H\}$ NMR signal was observed at δ_P 11.6, shifted downfield with respect to triazolium salt **19** (δ_P −19.8).

The molecular structure of complex **20**·C_6H_{14} is presented in Fig. 12. The compound is indeed a "square planar" Pd(II) complex, albeit distorted due to spatial constraints imposed by the *trans*-chelating phosphinocarbene ligand. The coordination environment is bent along both diagonals (P1–Pd1–C1 = 160.08(4)°, Cl1–Pd1–Cl2 = 169.18(2)°), which is reflected in the τ_4 index[62] of 0.22 that suggests angular distortion towards the tetrahedral geometry (ideal square and tetrahedron would yield τ_4 values of 0 and 1, respectively). Among the interligand angles, the P1–Pd1–Cl2 angle is opened to 98°, whereas the three remaining angles are approximately 88° (Table 4). The Pd-donor distances compare well with the parameters reported for *trans*-[$PdCl_2${$P(o\text{-tolyl})_3$}(L)] (L = 3-methyl-1,4-diphenyltriazol-5-ylidene), which is a complex with a similar geometry and donor set.[63]

Compared with triazole **17**, the ferrocene unit in **20**·C_6H_{14} is slightly more tilted (dihedral angle 6.49(9)°) and, mainly,

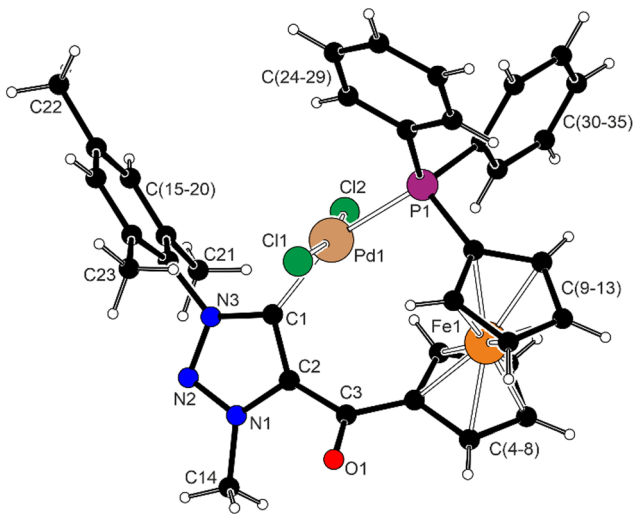

Fig. 12 Complex in the structure of **20**·C_6H_{14}. The selected distances and angles (in Å and °): Fe–C (range) 2.041(2)–2.075(2), P1–C9 1.813(2), P1–C24 1.816(2), P1–C30 1.824(1), C3–O1 1.224(2), C1–C2 1.386(2), C2–N1 1.366(2), N1–N2 1.312(2), N2–N3 1.337(2), and N3–C1 1.360(2). A displacement ellipsoid plot is available in the ESI.†

Table 4 Coordination geometry parameters for **20**·C_6H_{14}

Distances [Å]		Angles[a] [°]	
Pd1–P1	2.3239(5)	P1–Pd1–Cl1	88.70(2)
Pd1–C1	2.003(1)	P1–Pd1–Cl2	98.26(2)
Pd1–Cl1	2.3036(5)	C1–Pd1–Cl1	87.33(4)
Pd1–Cl2	2.3100(5)	C1–Pd1–Cl2	88.81(4)

[a] The sum of the interligand angles is 363.10°.

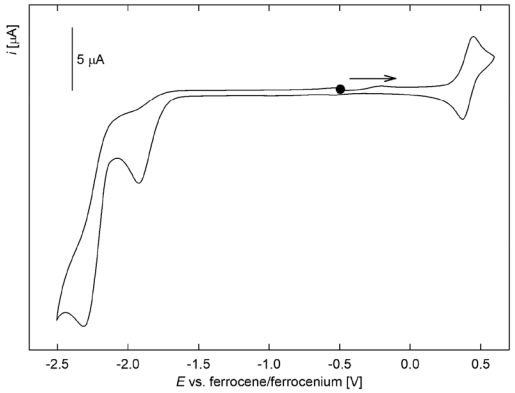

Fig. 13 Cyclic voltammograms (anodic branches) of complex **20** (recorded in 0.1 M $Bu_4N[PF_6]/CH_2Cl_2$ at a glassy carbon disc electrode and a 100 mV s^{-1} scan rate).

less opened (τ = −68.5(1)°), approaching the ideal synclinal eclipsed conformation (τ = 72°)[64] to enable chelate coordination. The triazolylidene ring is twisted by 52.39(9)° from the plane of the cyclopentadienyl ring C(5–9), and the terminal mesityl ring is oriented perpendicularly to both the C_2N_3 ring and the mean coordination plane {Pd1,P1,Cl1,Cl2,C1} (interplanar angles: 84.11(8)° and 84.59(5)°, respectively).

The cyclic voltammogram of **20** (Fig. 13) revealed one reversible oxidation at 0.41 V, which was attributed to the ferrocene-based redox event. The oxidation occurs at more positive potentials than for the nonchelating carbene complexes (*vide supra*), which corresponds to the electron-withdrawing nature of the additional substituent (PPh_2) at the ferrocene unit, which is further enhanced by its coordination. In the cathodic region, complex **20** underwent two successive irreversible reductions at approximately −1.92 and −2.32 V, similar to those observed for the Group 11 metal complexes discussed above.

Conclusions

We describe the synthesis of acyltriazolylidene complexes, which most likely represent the first compounds of this type. The proligand for these complexes, 4-acyltriazolium salt **3**, was obtained smoothly *via* a Cu-catalysed [3 + 2]-cycloaddition reaction from mesityl azide and ferrocenyl ethynyl ketone (FcC(O)C≡CH) followed by alkylation of the formed triazole with Meerwein salt. The triazolium salt was converted to a series of Group 11 metal complexes, either homoleptic $[ML_2][BF_4]$ (M = Cu, Ag, or Au) or with an auxiliary chloride ligand, [LMCl] (M = Cu or Au). These compounds were structurally characterised by a combination of spectroscopic methods and single-crystal X-ray diffraction analysis, and their catalytic properties were probed for the cyclisation of *N*-propargylbenzamide to the respective methylenoxazoline. Considering the presence of the redox-active ferrocenyl group, the compounds were further studied by voltammetric techniques, which revealed reversible ferrocene/ferrocenium transitions and irreversible reductions presumably localised at the carbene fragment. The ^{13}C NMR and electrochemical data obtained for a pair of Pd(II) bis-carbene complexes with or without the C═O linker and 1,3-diisopropyl-1,3-dihydro-2*H*-benzimidazol-2-ylidene ligand as the reporter moiety indicated that the carbonyl groups render both ligand parts (*i.e.*, the ferrocene unit and the triazolylidene unit) less electron rich, thereby decreasing the ligand's σ donation ability.

Finally, a similar synthetic strategy (albeit with additional protection/deprotection steps required to preserve the reactive phosphine moiety) and direct Ag-to-Pd transmetalation were used to prepare Pd(II) complex **20**, which is a rare example of a complex that features a *trans*-spanning P,C-ligand.

Data availability

The data supporting this article have been included as part of the extensive ESI.† The crystallographic data for all the structures have been deposited with the Cambridge Crystallographic Data Centre under deposition numbers CCDC 2427432–2427441.†

Conflicts of interest

There are no conflicts to declare.

Acknowledgements

This work was supported by the Czech Science Foundation (project no. 23-06718S).

References

1 (*a*) H.-W. Wanzlick and E. Schikora, *Angew. Chem.*, 1960, **72**, 494; (*b*) H.-W. Wanzlick and E. Schikora, *Chem. Ber.*, 1961, **94**, 2389; (*c*) H.-W. Wanzlick, *Angew. Chem., Int. Ed. Engl.*, 1962, **1**, 75.
2 (*a*) K. Öfele, *J. Organomet. Chem.*, 1968, **12**, P42 See also: (*b*) D. J. Cardin, B. Cetinkaya and M. F. Lappert, *Chem. Rev.*, 1972, **72**, 545; (*c*) M. F. Lappert, *J. Organomet. Chem.*, 1988, **358**, 185.
3 W. Kirmse, *Angew. Chem., Int. Ed.*, 2010, **49**, 8798.
4 (*a*) A. J. Arduengo, R. L. Harlow and M. Kline, *J. Am. Chem. Soc.*, 1991, **113**, 361; (*b*) A. J. Arduengo, H. V. R. Dias, R. L. Harlow and M. Kline, *J. Am. Chem. Soc.*, 1992, **114**, 5530; (*c*) A. J. Arduengo, J. R. Goerlich and W. J. Marshall, *J. Am. Chem. Soc.*, 1995, **117**, 11027.
5 The first isolable carbene, $R_2PCSiMe_3$, was reported earlier in: A. Igau, H. Grützmacher, A. Baceiredo and G. Bertrand, *J. Am. Chem. Soc.*, 1988, **110**, 6463.
6 (*a*) F. E. Hahn and M. C. Jahnke, *Angew. Chem., Int. Ed.*, 2008, **47**, 3122; (*b*) P. de Frémont, N. Marion and

S. P. Nolan, *Coord. Chem. Rev.*, 2009, **253**, 862; (*c*) D. J. Nelson and S. P. Nolan, *Chem. Soc. Rev.*, 2013, **42**, 6723; (*d*) M. N. Hopkinson, C. Richter, M. Schedler and F. Glorius, *Nature*, 2014, **510**, 485; (*e*) H. V. Huynh, *Chem. Rev.*, 2018, **118**, 9457; (*f*) P. Bellotti, M. Koy, M. N. Hopkinson and F. Glorius, *Nat. Rev. Chem.*, 2021, **5**, 711.

7 V. Nair, S. Bindu and V. Sreekumar, *Angew. Chem., Int. Ed.*, 2004, **43**, 5130.

8 (*a*) P. Mathew, A. Neels and M. Albrecht, *J. Am. Chem. Soc.*, 2008, **130**, 13534 For reviews, see: (*b*) O. Schuster, L. Yang, H. G. Raubenheimer and M. Albrecht, *Chem. Rev.*, 2009, **109**, 3445; (*c*) R. H. Crabtree, *Coord. Chem. Rev.*, 2013, **257**, 755; (*d*) G. Guisado-Barrios, M. Soleilhavoup and G. Bertrand, *Acc. Chem. Res.*, 2018, **51**, 3236; (*e*) Á. Vivancos, C. Segarra and M. Albrecht, *Chem. Rev.*, 2018, **118**, 9493; (*f*) R. Maity and B. Sarkar, *JACS Au*, 2022, **2**, 22.

9 R. H. Crabtree, *Coord. Chem. Rev.*, 2013, **257**, 755.

10 1,2,3-Triazoles are readily accessible by Cu-catalysed Huisgen cycloaddition from azides and alkynes: (*a*) M. Meldal and C. Wenzel Tornøe, *Chem. Rev.*, 2008, **108**, 2952; (*b*) M. Breugst and H.-U. Reissig, *Angew. Chem., Int. Ed.*, 2020, **59**, 12293.

11 (*a*) J. D. Crowley, A.-L. Lee and K. J. Kilpin, *Aust. J. Chem.*, 2011, **64**, 1118; (*b*) K. F. Donnelly, A. Petronilho and M. Albrecht, *Chem. Commun.*, 2013, **49**, 1145; (*c*) S. A. Patil, H. M. Heras-Martinez, A. M. Lewis, S. A. Patil and A. Bugarin, *Polyhedron*, 2021, **194**, 114935; (*d*) G. Guisado-Barrios, M. Soleilhavoup and G. Bertrand, *Acc. Chem. Res.*, 2018, **51**, 3236; (*e*) W. Stroek and M. Albrecht, *Chem. Soc. Rev.*, 2024, **53**, 6322 and ref. 8*e* and *f*.

12 (*a*) B. Bildstein, *J. Organomet. Chem.*, 2001, **617–618**, 28; (*b*) U. Siemeling, *Eur. J. Inorg. Chem.*, 2012, 3523.

13 P. Štěpnička, *Dalton Trans.*, 2022, **51**, 8085.

14 (*a*) L. Hettmanczyk, S. Manck, C. Hoyer, S. Hohloch and B. Sarkar, *Chem. Commun.*, 2015, **51**, 10949; (*b*) L. Hettmanczyk, L. Suntrup, S. Klenk, C. Hoyer and B. Sarkar, *Chem. – Eur. J.*, 2017, **23**, 576; (*c*) D. Aucamp, T. Witteler, F. Dielmann, S. Siangwata, D. C. Liles, G. S. Smith and D. I. Bezuidenhout, *Eur. J. Inorg. Chem.*, 2017, 1227; (*d*) S. Klenk, S. Rupf, L. Suntrup, M. van der Meer and B. Sarkar, *Organometallics*, 2017, **36**, 2026; (*e*) C. Hoyer, P. Schwerk, L. Suntrup, J. Beerhues, M. Nössler, U. Albold, J. Dernedde, K. Tedin and B. Sarkar, *Eur. J. Inorg. Chem.*, 2021, 1373 For similar compounds containing ferrocenyl and/or cobaltocenyl subsituents, see: (*f*) S. Vanicek, M. Podewitz, J. Stubbe, D. Schulze, H. Kopacka, K. Wurst, T. Müller, P. Lippmann, S. Haslinger, H. Schottenberger, K. R. Liedl, I. Ott, B. Sarkar and B. Bildstein, *Chem. – Eur. J.*, 2018, **24**, 3742.

15 (*a*) R. Haraguchi, S. Hoshino, T. Yamazaki and S. Fukuzawa, *Chem. Commun.*, 2018, **54**, 2110; (*b*) R. Haraguchi, T. Yamazaki, K. Torita, T. Ito and S. Fukuzawa, *Dalton Trans.*, 2020, **49**, 17578.

16 D. Aucamp, S. V. Kumar, D. C. Liles, M. A. Fernandes, L. Harmse and D. I. Bezuidenhout, *Dalton Trans.*, 2018, **47**, 16072.

17 This contrasts with the situation encountered among imidazol-2-ylidene and related ligands, where compounds with ferrocenylmethyl substituents dominate due to their facile synthesis; see ref. 12*b*. Selected recent examples: (*a*) K. Arumugam, J. Chang, V. M. Lynch and C. W. Bielawski, *Organometallics*, 2013, **32**, 4334; (*b*) K. Arumugam, C. D. Varnado, S. Sproules, V. M. Lynch and C. W. Bielawski, *Chem. – Eur. J.*, 2013, **19**, 10866; (*c*) P. He, Y. Du, S. Wang, C. Cao, X. Wang, G. Pang and Y. Shi, *Z. Anorg. Allg. Chem.*, 2013, **639**, 1004; (*d*) H. A. Özbek, P. S. Aktaş, J.-C. Daran, M. Oskay, F. Demirhan and B. Çetinkaya, *Inorg. Chim. Acta*, 2014, **423**, 435; (*e*) J. F. Arambula, R. McCall, K. J. Sidoran, D. Magda, N. A. Mitchell, C. W. Bielawski, V. M. Lynch, J. L. Sesslerg and K. Arumugam, *Chem. Sci.*, 2016, **7**, 1245; (*f*) G. L. Reinhard, S. Jayaraman, J. W. Prybil, J. F. Arambula and K. Arumugam, *Dalton Trans.*, 2022, **51**, 1533.

18 (*a*) K. Škoch, I. Císařová, F. Uhlík and P. Štěpnička, *Dalton Trans.*, 2018, **47**, 16082; (*b*) K. Škoch, J. Schulz, I. Císařová and P. Štěpnička, *Organometallics*, 2019, **38**, 3060; (*c*) K. Škoch, P. Vosáhlo, I. Císařová and P. Štěpnička, *Dalton Trans.*, 2020, **49**, 1011; (*d*) M. Franc, J. Schulz and P. Štěpnička, *Dalton Trans.*, 2024, **53**, 11445.

19 (Ferrocenylcarbonyl)triazoles are also rare and have been studied as redox-active organometalic tags in the preparation of new biologically active compounds and modification of self-assembled surfaces: (*a*) K. Kowalczyk, A. Błauż, W. M. Ciszewski, A. Wieczorek, B. Rychlik and D. Plażuk, *Dalton Trans.*, 2017, **46**, 17041; (*b*) K. Chrabąszcz, A. Błauż, M. Gruchała, M. Wachulec, B. Rychlik and D. Plażuk, *Chem. – Eur. J.*, 2021, **27**, 6254; (*c*) J. P. Collman, N. K. Devaraj and C. E. D. Chidsey, *Langmuir*, 2004, **20**, 1051.

20 (*a*) P. Vosáhlo, J. Schulz, I. Císařová and P. Štěpnička, *Dalton Trans.*, 2021, **50**, 6232; (*b*) P. Vosáhlo, I. Císařová and P. Štěpnička, *New J. Chem.*, 2022, **46**, 21536; (*c*) P. Vosáhlo and P. Štěpnička, *New J. Chem.*, 2023, **47**, 4510.

21 Correspondingly, only a handful of the related compounds featuring the more common imidazole-2-ylidene with *N*-acyl and similar substituents (*e.g.*, ester or carbamoyl) have been reported: (*a*) F. Bonati, A. Burini, B. R. Pietroni and B. Bovio, *J. Organomet. Chem.*, 1991, **408**, 271; (*b*) B. Bovio, A. Burini and B. R. Pietroni, *J. Organomet. Chem.*, 1993, **452**, 287; (*c*) G. E. Dobereiner, C. A. Chamberlin, N. D. Schley and R. H. Crabtree, *Organometallics*, 2010, **29**, 5728; (*d*) M. Jonek, A. Makhloufi, P. Rech, W. Frank and C. Ganter, *J. Organomet. Chem.*, 2014, **750**, 140.

22 Selected examples: (*a*) H. Seo, H. Park, B. Y. Kim, J. H. Lee, S. U. Son and Y. K. Chang, *Organometallics*, 2003, **22**, 618; (*b*) S. Gischig and A. Togni, *Organometallics*, 2004, **23**, 2479; (*c*) S. Gischig and A. Togni, *Organometallics*, 2005, **24**, 203; (*d*) F. Visentin and A. Togni, *Organometallics*, 2007, **26**, 3746; (*e*) A. Labande, J.-C. Daran, E. Manoury and R. Poli, *Eur. J. Inorg. Chem.*, 2007, 1205; (*f*) J. Shi, P. Yang, Q. Tong

and L. Jia, *Dalton Trans.*, 2008, 938; (*g*) S. Gülcemal, A. Labande, J.-C. Daran, B. Çetinkaya and R. Poli, *Eur. J. Inorg. Chem.*, 2009, 1806; (*h*) N. Debono, A. Labande, E. Manoury, J.-C. Daran and R. Poli, *Organometallics*, 2010, **29**, 1879; (*i*) J. Csizmadiová, M. Mečiarová, A. Almássy, B. Horváth and R. Šebesta, *J. Organomet. Chem.*, 2013, **737**, 47; (*j*) A. Labande, N. Debono, A. Sournia-Saquet, J.-C. Daran and R. Poli, *Dalton Trans.*, 2013, **42**, 6531; (*k*) P. Loxq, N. Debono, S. Gülcemal, J.-C. Daran, E. Manoury, R. Poli, B. Çetinkaya and A. Labande, *New J. Chem.*, 2014, **38**, 338; (*l*) P. Loxq, J.-C. Daran, E. Manoury, R. Poli and A. Labande, *Eur. J. Inorg. Chem.*, 2015, 609; (*m*) Y. D. Lahneche, A. Lachguar, C. Mouton, J.-C. Daran, E. Manoury, R. Poli, M. Benslimane, A. Labande and E. Deydier, *Inorg. Chim. Acta*, 2019, **492**, 91.

23 S. Barriga, C. F. Marcos, O. Riant and T. Torroba, *Tetrahedron*, 2002, **58**, 9785.

24 (*a*) D. Font, C. Jimeno and M. A. Pericàs, *Org. Lett.*, 2006, **8**, 4653; (*b*) D. Giguère, R. Patnam, M.-A. Bellefleur, C. St-Pierre, S. Sato and R. Roy, *Chem. Commun.*, 2006, 2379.

25 K. Nakamoto, *Infrared and Raman Spectra of Inorganic and Coordination Compounds, Part A: Theory and Applications in Inorganic Chemistry*, Wiley, Hoboken, 6th edn, 2009, ch. 2.6.1, pp. 192–204.

26 K. M. Steed and J. W. Steed, *Chem. Rev.*, 2015, **115**, 2895.

27 For examples of reactions of azolium salts with Ag_2O leading to carbene complexes, see: (*a*) H. M. J. Wang and I. J. B. Lin, *Organometallics*, 1998, **17**, 972; (*b*) R. Heath, H. Müller-Bunz and M. Albrecht, *Chem. Commun.*, 2015, **51**, 8699.

28 Selected examples: (*a*) C. Mejuto, G. Guisado-Barrios, D. Gusev and E. Peris, *Chem. Commun.*, 2015, **51**, 13914; (*b*) R. Pretorius, M. R. Fructos, H. Müller-Bunz, R. A. Gossage, P. J. Pérez and M. Albrecht, *Dalton Trans.*, 2016, **45**, 14591; (*c*) J. R. Wright, P. C. Young, N. T. Lucas, A.-L. Lee and J. D. Crowley, *Organometallics*, 2013, **32**, 7065 and ref. 32*b* and 33*b*.

29 For examples of Ag-to-Cu transmetalation in similar systems, see: (*a*) H. Iwasaki, Y. Teshima, Y. Yamada, R. Ishikawa, Y. Koga and K. Matsubara, *Dalton Trans.*, 2016, **45**, 5713; (*b*) S. Hohloch, L. Suntrup and B. Sarkar, *Inorg. Chem. Front.*, 2016, **3**, 67; (*c*) T. Nakamura, T. Tareshima, K. Ogata and S. Fukuzawa, *Org. Lett.*, 2011, **13**, 620; (*d*) A. Petronilho, H. Müller-Bunz and M. Albrecht, *Chem. Commun.*, 2012, **48**, 6499.

30 B. Cordero, V. Gómez, A. E. Platero-Prats, M. Revés, J. Echeverría, E. Cremades, F. Barragán and S. Alvarez, *Dalton Trans.*, 2008, 2832.

31 P. Pyykkö, *Chem. Rev.*, 1988, **88**, 563.

32 (*a*) S. Hohloch, D. Scheiffele and B. Sarkar, *Eur. J. Inorg. Chem.*, 2013, 3956; (*b*) L. Hettmanczyk, S. J. P. Spall, S. Klenk, M. van der Meer, S. Hohloch, J. A. Weinstein and B. Sarkar, *Eur. J. Inorg. Chem.*, 2017, 2112; (*c*) F. Lazreg, M. Vasseur, A. M. Z. Slawin and C. S. J. Cazin, *Beilstein J. Org. Chem.*, 2020, **16**, 482; (*d*) J. F. Schlagintweit, C. H. G. Jakob, N. L. Wilke, M. Ahrweiler, C. Frias, J. Frias, M. König, E.-M. H. J. Esslinger, F. Marques, J. F. Machado, R. M. Reich, T. S. Morais, J. D. G. Correia, A. Prokop and F. E. Kühn, *J. Med. Chem.*, 2021, **64**, 15747.

33 (*a*) H. Inomata, K. Ogata, S. Fukuzawa and Z. Hou, *Org. Lett.*, 2012, **14**, 3986; (*b*) L. Hettmanczyk, D. Schulze, L. Suntrup and B. Sarkar, *Organometallics*, 2016, **35**, 3828.

34 (*a*) T. G. Appleton, H. C. Clark and L. E. Manzer, *Coord. Chem. Rev.*, 1973, **10**, 335; (*b*) F. R. Hartley, *Chem. Soc. Rev.*, 1973, **2**, 163; (*c*) S. Fuertes, A. J. Chueca and V. Sicilia, *Inorg. Chem.*, 2015, **54**, 9885.

35 (*a*) G. Gritzner and J. Kůta, *Pure Appl. Chem.*, 1984, **56**, 461; (*b*) R. R. Gagné, C. A. Koval and G. C. Lisensky, *Inorg. Chem.*, 1980, **19**, 2854.

36 P. Zanello, *Inorganic Electrochemistry, Theory, Practice and Application*, The Royal Society of Chemistry, Cambridge, 2003, ch. 2, pp. 110–115.

37 (*a*) H. V. Huynh, Y. Han, R. Jothibasu and J. A. Yang, *Organometallics*, 2009, **28**, 5395; (*b*) Q. Teng and H. V. Huynh, *Dalton Trans.*, 2017, **46**, 614; (*c*) H. V. Huynh, *Chem. Rev.*, 2018, **118**, 9457.

38 H. V. Huynh, Y. Han, J. H. H. Ho and G. K. Tan, *Organometallics*, 2006, **25**, 3267.

39 Ferrocene displays an absorption band at 440 nm (in EtOH and gas phase): (*a*) D. R. Scott and R. S. Becker, *J. Chem. Phys.*, 1961, **35**, 516; (*b*) A. T. Armstrong, F. Smith, E. Elder and S. P. McGlynn, *J. Chem. Phys.*, 1967, **46**, 4321.

40 (*a*) D. Yuan and H. V. Huynh, *Organometallics*, 2012, **31**, 405; (*b*) J. R. Wright, P. C. Young, N. T. Lucas, A.-L. Lee and J. D. Crowley, *Organometallics*, 2013, **32**, 7065.

41 D. A. Khobragade, S. G. Mahamulkar, L. Pospíšil, I. Císařová, L. Rulíšek and U. Jahn, *Chem. – Eur. J.*, 2012, **18**, 12267.

42 C. Hansch, A. Leo and R. W. Taft, *Chem. Rev.*, 1991, **91**, 165.

43 (*a*) A. S. K. Hashmi, J. P. Weyrauch, W. Frey and J. W. Bats, *Org. Lett.*, 2004, **6**, 4391; (*b*) A. S. K. Hashmi, M. Rudolph, S. Schymura, J. Visus and W. Frey, *Eur. J. Org. Chem.*, 2006, 4905; (*c*) A. S. K. Hashmi, A. M. Schuster and F. Rominger, *Angew. Chem., Int. Ed.*, 2009, **48**, 8247; (*d*) J. P. Weyrauch, A. S. K. Hashmi, A. Schuster, T. Hengst, S. Schetter, A. Littmann, M. Rudolph, M. Hamzic, J. Visus, F. Rominger, W. Frey and J. W. Bats, *Chem. – Eur. J.*, 2010, **16**, 956; (*e*) O. Bárta, I. Císařová, J. Schulz and P. Štěpnička, *New J. Chem.*, 2019, **43**, 11258.

44 Although insoluble AgCl separated upon mixing **5** with $AgNTf_2$, a possible Au–Ag cooperativity cannot be ruled out entirely. For examples, see: (*a*) D. Wang, R. Cai, S. Sharma, J. Jirak, S. K. Thummanapelli, N. G. Akhmedov, H. Zhang, X. Liu, J. L. Petersen and X. Shi, *J. Am. Chem. Soc.*, 2012, **134**, 9012; (*b*) Z. Lu, J. Han, G. B. Hammon and B. Xu, *Org. Lett.*, 2015, **17**, 4534.

45 Changing the redox state of the ferrocene unit in [AuCl(L)] complexes with type **B** ligands (but with a soluble ferrocenium salt as an oxidant) was shown to influence catalytic activity in this particular cyclisation reaction (see ref. 14*d*).

46 (*a*) Y. G. Gololobov, I. N. Zhmurova and L. F. Kasukhin, *Tetrahedron*, 1981, **37**, 437; (*b*) Y. G. Gololobov and L. F. Kasukhin, *Tetrahedron*, 1992, **48**, 1353.

47 K. Škoch, I. Císařová, J. Schulz, U. Siemeling and P. Štěpnička, *Dalton Trans.*, 2017, **46**, 10339.
48 J. M. Brunel, B. Faure and M. Maffei, *Coord. Chem. Rev.*, 1998, **178–180**, 665.
49 M. Van Overschelde, E. Vervecken, S. G. Modha, S. Cogen, E. Van der Eycken and J. Van der Eycken, *Tetrahedron*, 2009, **65**, 6410.
50 (*a*) T. R. Ward, L. M. Venanzi, A. Albinati, F. Lianza, T. Gerfin, V. Gramlich and G. M. R. Tombo, *Helv. Chim. Acta*, 1991, **74**, 983; (*b*) T. Imamoto, M. Matsuo, T. Nonomura, K. Kishikawa and M. Yanagawa, *Heteroat. Chem.*, 1993, **4**, 475.
51 J. Podlaha, P. Štěpnička, J. Ludvík and I. Císařová, *Organometallics*, 1996, **15**, 543.
52 H. Brisset, Y. Gourdel, P. Pellon and M. Le Corre, *Tetrahedron Lett.*, 1993, **34**, 4523.
53 P. Štěpnička and I. Císařová, *Dalton Trans.*, 2013, **42**, 3373.
54 G. Gasser, A. J. Fischmann, C. M. Forsyth and L. Spiccia, *J. Organomet. Chem.*, 2007, **692**, 3835.
55 For related examples, see: (*a*) G. Ferguson, J. F. Gallagher, C. Glidewell and C. M. Zakaria, *Acta Crystallogr., Sect. C: Cryst. Struct. Commun.*, 1993, **49**, 967; (*b*) G. Ferguson, J. F. Gallagher, C. Glidewell and C. M. Zakaria, *J. Organomet. Chem.*, 1994, **464**, 95; (*c*) J. F. Gallagher, G. Ferguson, C. Glidewell and C. M. Zakaria, *Acta Crystallogr., Sect. C: Cryst. Struct. Commun.*, 1994, **50**, 18; (*d*) Y. Li, G. Ferguson, C. Glidewell and C. M. Zakaria, *Acta Crystallogr., Sect. C: Cryst. Struct. Commun.*, 1994, **50**, 857.
56 (*a*) P. Štěpnička and T. Baše, *Inorg. Chem. Commun.*, 2001, **4**, 682; (*b*) P. Štěpnička and I. Císařová, *New J. Chem.*, 2002, **26**, 1389.
57 S. I. Kirin, H.-B. Kraatz and N. Metzler-Nolte, *Chem. Soc. Rev.*, 2006, **35**, 348.
58 The torsion angle C4–Cg1–Cg2–C9 is given, where Cg1 and Cg2 are the centroids of the cyclopentadienyl rings C(4–8) and C(9–13), respectively (analogously for molecule 2). .
59 (*a*) Z. Freixa and P. W. N. M. van Leeuwen, *Coord. Chem. Rev.*, 2008, **252**, 1755; (*b*) C. A. Bessel, P. Aggarwal, A. C. Marschilok and K. J. Takeuchi, *Chem. Rev.*, 2001, **101**, 1031.
60 Representative examples: (*a*) I. R. Butler, M. Kalaji, L. Nehrlich, M. Hursthouse, A. I. Karaulov and K. M. A. Malik, *J. Chem. Soc., Chem. Commun.*, 1995, 459; (*b*) K. Tani, M. Yabuta, S. Nakamura and T. Yamagata, *J. Chem. Soc., Dalton Trans.*, 1993, 2781; (*c*) J. Kühnert, M. Dušek, J. Demel, H. Lang and P. Štěpnička, *Dalton Trans.*, 2007, 2802; (*d*) P. Štěpnička, B. Schneiderová, J. Schulz and I. Císařová, *Organometallics*, 2013, **32**, 5754; (*e*) J. Tauchman, I. Císařová and P. Štěpnička, *Dalton Trans.*, 2014, **43**, 1599; (*f*) L. Wang, M. Chen, P. Zhang, W. Li and J. Zhang, *J. Am. Chem. Soc.*, 2018, **140**, 3467.
61 T. E. Schmid, D. C. Jones, O. Songis, O. Diebolt, M. R. L. Furst, A. M. Z. Slawin and C. S. J. Cazin, *Dalton Trans.*, 2013, **42**, 7345.
62 L. Yang, D. R. Powell and R. P. Houser, *Dalton Trans.*, 2007, 955.
63 A. Dasgupta, V. Ramkumar and S. Sankararaman, *Eur. J. Org. Chem.*, 2016, 4817. The parameters were retrieved from the Cambridge Structural Database, refcode: IWUFAJ. The major difference between the compounds is the Pd–P bond length measuring 2.356 Å in the reference compound.
64 K.-S. Gan and T. S. A. Hor, in *Ferrocenes: Homogeneous Catalysis, Organic Synthesis Materials Science*, ed. A. Togni and T. Hayashi, Wiley-VCH, Weinheim, Germany, 1995, ch. 1, pp. 3–104.